Chapter 3

Low-Pressure Crystallization of Sol-Gel-Derived $PbZr_{0.52}Ti_{0.48}O_3$ Thin Films at Low Temperature for Low-Voltage Operation

3-1 Introduction

Lead zirconate titanate (PZT) thin films have received considerable research interest due to their excellent ferroelectric properties and low crystallization temperatures. Several methods, such as sputtering, sol-gel method, and metal organic chemical vapor deposition, are commonly employed for producing ferroelectric PZT thin films [33-35]. Among them, the sol-gel method has the advantages of precise composition control, simplicity, and lower cost over other techniques [34, 36]. However, a high-temperature post deposition annealing step is normally required to transform as-deposited thin films into the desirable perovskite structure. This relatively high-temperature step (about 650 ^{o}C) imposes a severe constraint on the minimum process temperature and renders the sol-gel method unsuitable for embedded ferroelectric random access memory (FRAM) applications. To lower the crystallization temperature of PZT thin films, two-step low-pressure annealing has been previously proposed [36]. The removal of residual gases (e.g., CO_2 and H_2O) by the low-pressure annealing was credited for the reduced crystallization temperature and improved ferreoelectric properties. Nevertheless, the reported crystallization temperature of 550°C was still too high for many embedded memory applications. Concurrently, it has been reported that the pyrochlore ($A_2B_2O_{7-X}$) phase is more stable than the perovskite (ABO_3) phase in oxygen-rich ambient, and that the complete phase transformation temperature indeed depends on O_2 partial pressure in the ambient [37, 38]. High oxygen partial pressure tends to stabilize the pyrochlore phase, while low oxygen partial pressure promotes the transformation to the perovskite structure [38].

In this study, we have successfully fabricated 120-nm-thick PZT thin films with well-saturated polarization behavior at a bias of 2 V using one-step low-pressure rapid thermal annealing (LP-RTA) at 500°C. Based on the Auger depth profiles and thermal desorption spectra obtained, we speculate that less incorporation of oxygen, and CO_2 and H_2O residues in the resultant films contributes to the formation of well-crystallized perovskite PZT thin films at a low annealing temperature. Moreover, the dielectric and electrical properties of

those films were addressed.

3-2. Experiments

The sol-gel-derived PZT films were deposited onto Pt/Ti/SiO_2/Si substrates. Precursor solutions were prepared from lead acetate trihydrate, $Pb(CH_3COO)_2 \cdot 3H_2O$, zirconium-n-propoxide, $Zr(C_3H_7O)_4$, titanium tetraisopropoxide, $Ti((CH_3)_2CHO)_4$. 2-methoxyethanal [$C_3H_8O_2$] was used as the solvent. Zr/Ti ratio in all solutions was maintained at 52/48, while Pb content, i.e., Pb/(Zr+Ti), was kept at 1.30 to compensate for the expected Pb loss during processing. The synthesized flowchart of precursor solutions was shown in Fig.2-1 (chapter 2). After precursor preparation, the spin-coated wafers were subjected to drying at 150°C for 10 min and then pyrolyzed at 400°C for 20 min in oxygen ambient. The target film thickness of about 120nm was achieved through multiple repetitions of the process sequence. Next, the deposited films were crystallized at 500°C for 15 min by rapid thermal annealing (RTA) at various pressures, i.e., 1 atm, 200 mbar, and 60 mbar. 100-nm-thick Pt top electrodes were then deposited by electron beam evaporation on the PZT films through a shadow mask with an area of 4.8×10^{-4} cm^2. The hysteresis characteristics were measured by RT66A. The crystalline microstructures and crystallinity of the ferroelectric thin films were analyzed by atomic force microscopy (AFM) and X-ray diffraction (XRD). Finally, the element depth profile of the PZT films was studied by Auger electron spectrometry (AES), while the residual gases (e.g., CO_2, and H_2O) and contamination left in the bulk of the films were detected using thermal desorption spectra (TDS). The dielectric and electrical properties were determined using a HP 4284A LCR meter and a Keithley 4200 semiconductor characterization system, respectively.

3-3. Results and Discussions

The experimental procedures were mentioned in the previous section. In the following we will discuss the pressure effect on the ferroelectric properties of low-temperature crystallized PZT films. Their crystallinities and microstructures will also be compared. Additionally, depth profiles of PZT thin films annealed in various oxygen pressures will be characterized. Moreover, pressure effect on residual gases (i.e. CO_2, H_2O and O_2) left in the $PbZr_{0.52}Ti_{0.48}O_3$ films after crystallization were also discussed. Furthermore, the dielectric and electrical properties of those films were also addressed.

3-3-1. Ferroelectric property

Figure 3-1 shows the polarization-electric field (P-E) characteristics as a function of the applied voltage from 2 to 4V for $PbZr_{0.52}Ti_{0.48}O_3$ films annealed at 500°C at various O_2 pressures, i.e., 1 atm, 200 mbar, and 60mbar. It is apparent that with decreasing O_2 pressure, the remanent polarization of $PbZr_{0.52}Ti_{0.48}O_3$ films increases, while their coercive field decreases. The improvement of P-E hysteresis loops is concomitant with the decrease in annealing pressure, and indicates that $PbZr_{0.52}Ti_{0.48}O_3$ films crystallized at low O_2 pressure are more easily saturated at a bias of 2V. For the sample annealed in 60 mbar O_2 ambient, the remanent polarization ($2P_r$) can be as high as 36μC/cm^2 with a coercive field ($2E_C$) of 99.9kV/cm.

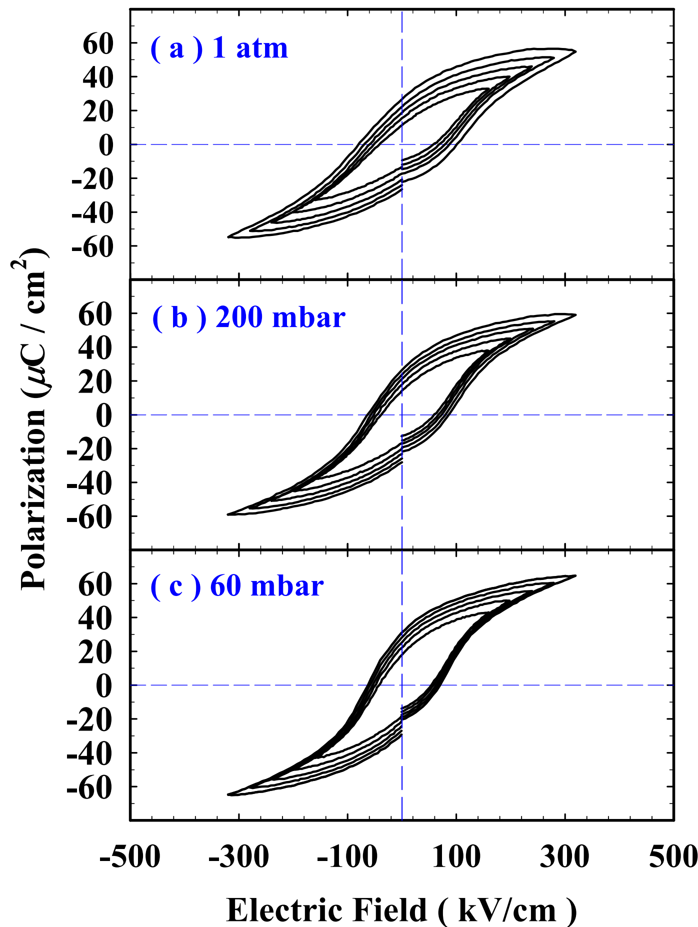

Fig. 3-1. *P-E* hysteresis loops of PZT thin films annealed in various oxygen pressures, (a) 1atm, (b) 200mbar, and (c) 60mbar. All samples were annealed at 500°C for 15min.

3-3-2. Crystallinity and Surface morphology

Figure 3-2 shows the corresponding surface morphologies obtained by atomic force microscopy (AFM) of the samples shown in Fig. 3-1. Samples crystallized at 550°C in 1 atm O_2 ambient are also shown for comparison. It can be seen that the grains become larger and more uniform with decreasing crystallization pressure. As a result, the microstructures of the $PbZr_{0.52}Ti_{0.48}O_3$ thin films annealed in low-pressure oxygen ambient are comparable to those annealed at 550°C in atmospheric oxygen. This indicates that the one-step low-pressure oxygen annealing technique can lower the $PbZr_{0.52}Ti_{0.48}O_3$ crystallization temperature by 50°C without causing degradation of ferroelectric properties. The reduction of the crystallization temperature is thought to arise from the inherent feature of the precursor, which is different from that used in Ref. [36] and the reported dependence of phase transformation temperature on oxygen pressure. Oxygen-rich ambient can help stabilize the pyrochlore phase. With decreasing oxygen pressure, the transformation from the pyrochlore phase to the perovskite

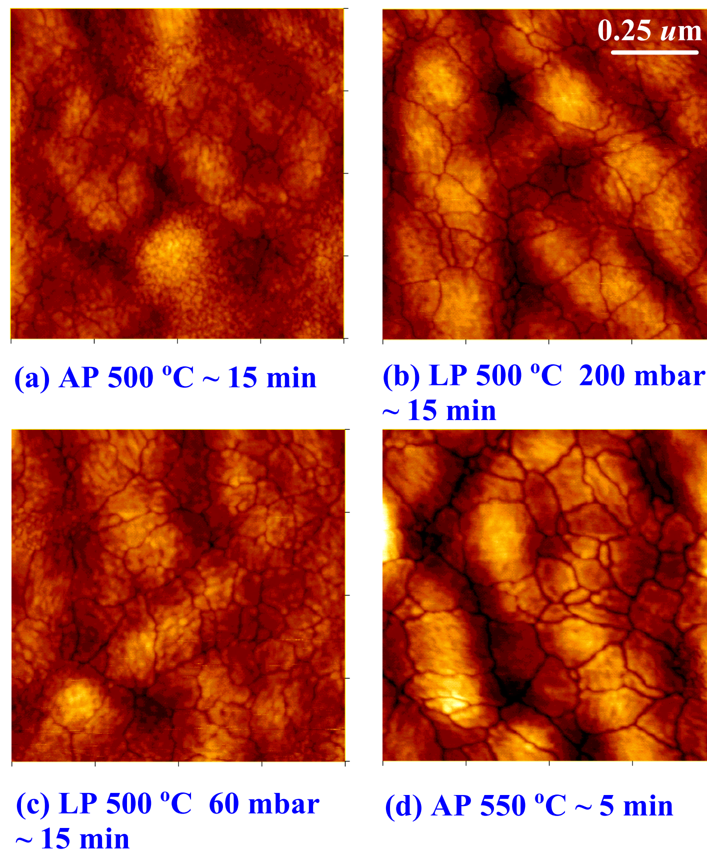

Fig. 3-2. Surface morphologies of PZT thin films annealed in various oxygen pressures and temperatures, (a) 1 atm, 500°C for 15 min, (b) 200 mbar, 500°C for 15 min, (c) 60mbar, 500°C for 15 min, and (d) 1 atm, 550°C for 5 min.

phase can occur at lower temperature [38]. It is worthy to note here that although a visible fraction of the nanocrystalline secondary phase on the perovskite phase was observed for samples annealed at atmospheric oxygen pressure [39], the signal of the secondary phase does not show up in X-ray diffraction spectra (shown in Fig. 3-3), indicating that the signal level of the secondary phase is below the resolution of the X-ray diffraction detector. The existence of the secondary phase at miniscule content is therefore speculated to be the culprit causing the degradation of ferroelectric properties of $PbZr_{0.52}Ti_{0.48}O_3$ thin films, as observed in the P-E loops.

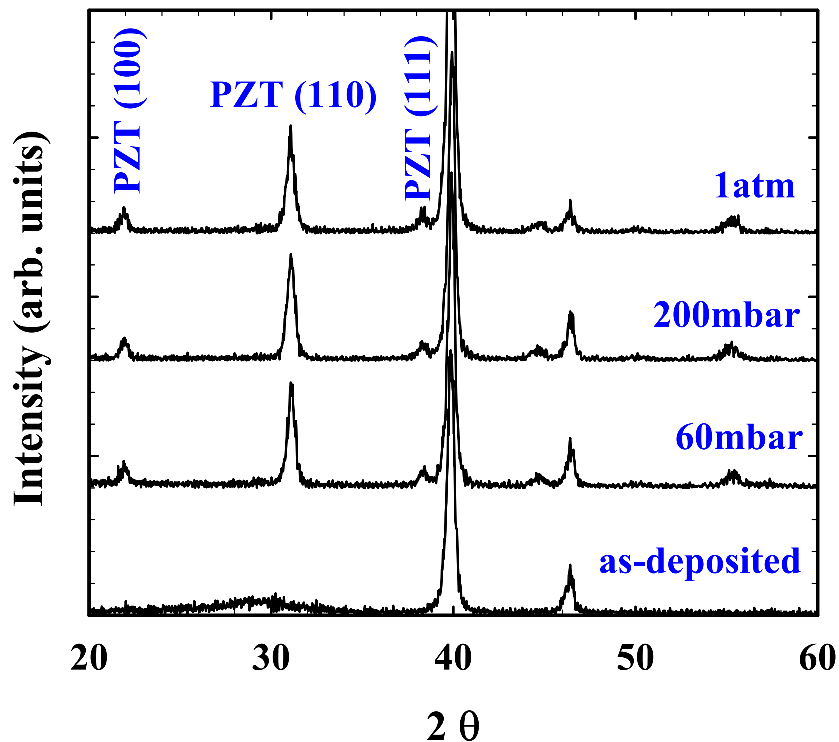

Fig. 3-3. X-ray diffraction patterns of PZT thin films annealed in various oxygen pressures at 500°C for 15min.

3-3-3. Interdiffusion property

The Auger electron spectroscopy (AES) depth profiles of the as-deposited $PZT/Pt/Ti/SiO_2/Si$ structures as well as of those annealed at $500^{o}C$ at various oxygen pressures are shown in Fig. 3-4. The oxygen concentration in the bulk of the PZT films subjected to 1 atm oxygen annealing was comparable to that in the as-deposited thin films, except at the PZT/Pt bottom electrode interface. The perturbed distribution is due to the interdiffusion between lead, titanium, zirconium, oxygen and platinum during heat treatment and is observed in all samples. The oxygen distribution for samples annealed in low-pressure

oxygen ambient is quite different from those annealed in 1 atm oxygen ambient, with the reduction in oxygen content in the bulk of the PZT thin films with decreasing oxygen pressure during annealing. This trend is consistent with the results of P-E loops. Auger depth profiles therefore support the hypothesis that the perovskite structure is preferred in low-pressure oxygen ambient. Besides the oxygen reduction in the bulk, additional oxygen loss near the top surface of the low-pressure-annealed PZT thin films is also observed. Fortunately, it seems not to be detrimental to the ferroelectric properties of the PZT thin films. This may be due to the fact that the interfacial layer is essentially covered by the Schottky depletion region [40].

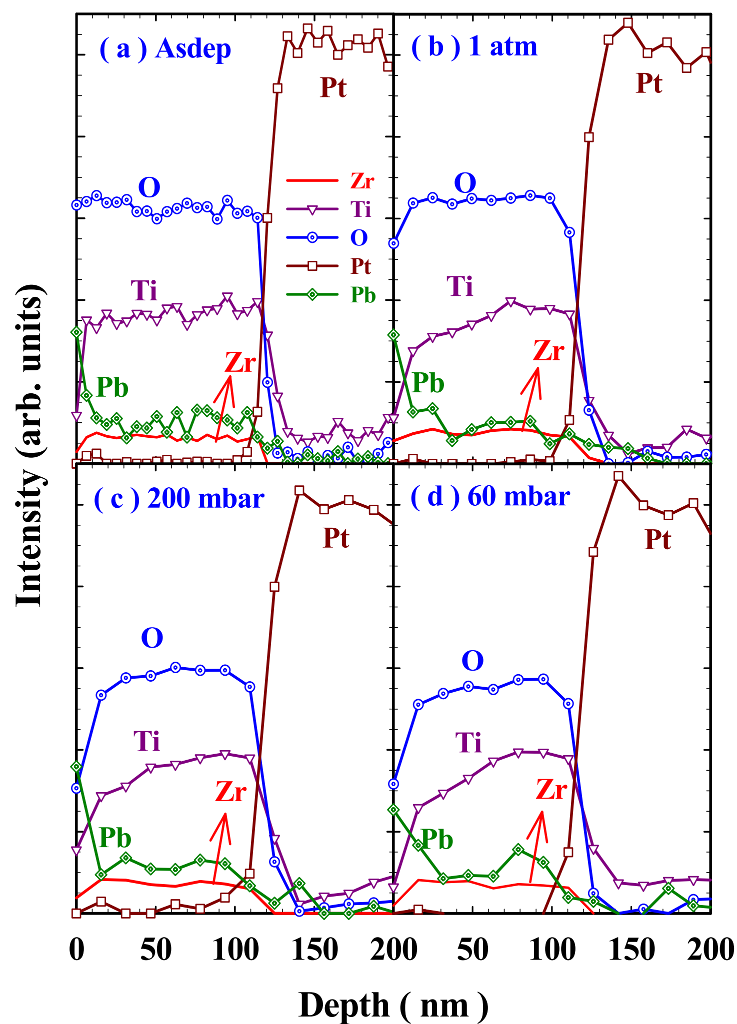

Fig. 3-4. AES depth profiles of as-deposited PZT thin films and those annealed in various oxygen pressures. All samples were annealed at 500°C for 15 min.

3-3-4. Thermal desorption property

Figure 3-5 shows the contents of residual gases, including CO_2, H_2O and O_2, left in the $PbZr_{0.52}Ti_{0.48}O_3$ films after crystallization by TDS. It can be seen that low-pressure annealing can reduce residual organics and contamination more effectively. Moreover, the emission of O_2 gas for the sample annealed at O_2 atmospheric pressure occurs at a lower temperature (i.e., around 495°C) than that annealed in low-pressure O_2 ambient. This suggests that atmospheric-pressure oxygen annealing results in abundant loosely bonded oxygen atoms in $PbZr_{0.52}Ti_{0.48}O_3$ thin films, which favors the formation of the pyrochlore structure [38], while low-pressure oxygen annealing effectively eliminates the oxygen content, as shown in Fig. 3-5(b), and thus promotes the formation of the more stable perovskite crystallization in $PbZr_{0.52}Ti_{0.48}O_3$ thin films. By reducing the residue and oxygen contents, the one-step low-pressure technique can significantly improve the ferroelectric properties of the $PbZr_{0.52}Ti_{0.48}O_3$ thin films.

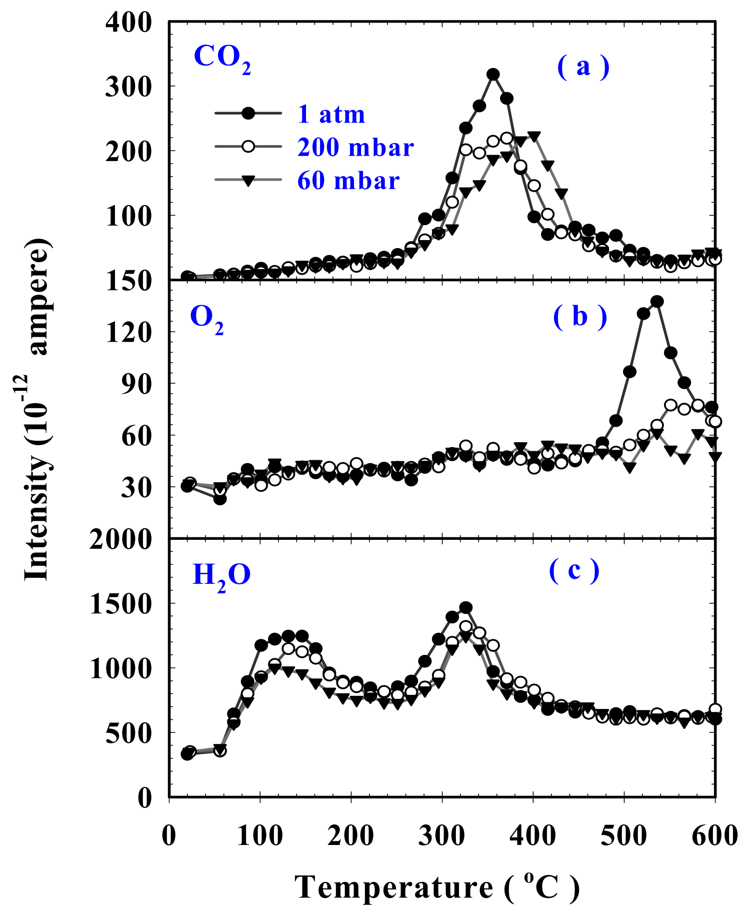

Fig. 3-5. TDS spectra of the PZT thin films annealed in various oxygen pressures. All samples were annealed at 500°C for 15 min.

3-3-5. Leakage property

To study further pressure effect of the electrical properties for those low-temperature-crystallized $PbZr_{0.52}Ti_{0.48}O_3$ thin films, the leakage current property was measured using a Keithley 4200 semiconductor characterization system. Figure 3-6 shows the leakage current density of those films annealed at 500°C for various oxygen pressures. For atmospheric-pressure crystallized $PbZr_{0.52}Ti_{0.48}O_3$ thin film, the leakage current was in the range of 10^{-6} A/cm^2, which is larger than that of annealed in low-pressure O_2 ambient (around 2.5×10^{-7} A/cm^2 at 2V). A breakdown behavior was found in the current-voltage characteristic at electrical field of around 150 kV/cm. This breakdown behavior and high leakage property may result in the shape-distortion of P-E curves at high field region. The high leakage property may be attributed to loosely bonded oxygen atoms in $PbZr_{0.52}Ti_{0.48}O_3$ thin films and the existence of nanocrystalline secondary phase in microstructure of Fig. 3-2(a). By reducing the pressure of O_2 ambient, the improved leakage property was found even though the pressure was only about 200 mbar.

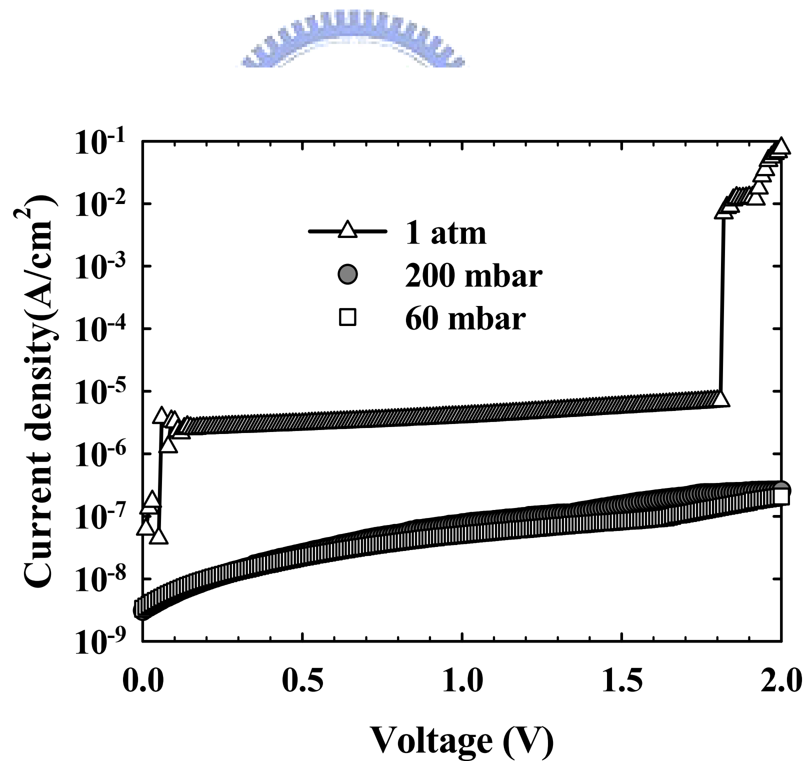

Fig. 3-6. Leakage current density-voltage characteristics of the PZT thin films annealed in various oxygen pressures. All samples were annealed at 500°C for 15 min.

3-3-6. Dielectric Property

Figure 3-7 displays the frequency dependence of dielectric constant (ε_r) and loss tangent (tan δ) of $PbZr_{0.52}Ti_{0.48}O_3$ thin films at 500°C at various oxygen pressures. The amplitude of the ac signal was 50 mV. The applied frequency was ranged from 100 Hz to 100 kHz. As can be seen, the dielectric constants of those films annealed at various oxygen pressures exhibit a slight decline while the applied frequency increased. The values of the loss tangent of these films keep below 0.050 from 100 Hz to 10 kHz. It was also found that the ε_r values of those films increased with decreasing the oxygen pressure. This implies that low-pressure crystallized $PbZr_{0.52}Ti_{0.48}O_3$ thin film exhibits a good crystallinity than that of atmospheric-pressure crystallized $PbZr_{0.52}Ti_{0.48}O_3$ thin film, resulting in a better insulative property.

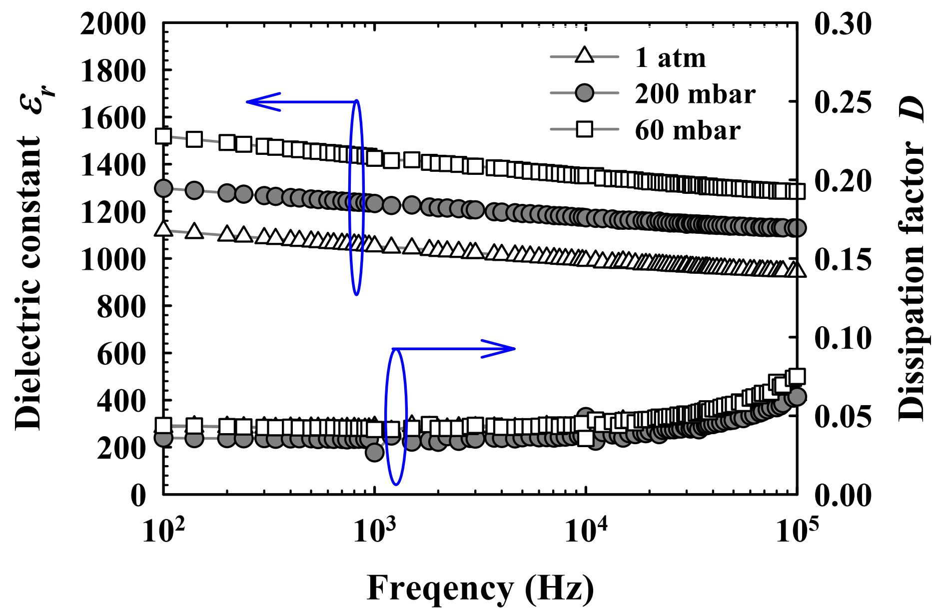

Fig. 3-7. Frequency-dependent dielectric properties of the PZT thin films annealed in various oxygen pressures. The signal level was about 50 mV. The frequency ranged form 100 Hz to 100 kHz. All samples were annealed at 500°C for 15 min.

Figure 3-8 shows the voltage dependence of small signal capacitance of $Pt/PbZr_{0.52}Ti_{0.48}O_3/Pt$ capacitors annealed at 500°C at various oxygen pressures. This capacitance-voltage (C-V) curves were recorded using an ac signal at 100 kHz and 50 mV amplitude with dc bias sweeping from -2.5 to 2.5 V then back to -2.5 V. For those ferroelectric capacitor annealed at various oxygen pressures, a butterfly-shape hysteresis appears in the

C-V curves. The applied small ac signal excited the vibration of non-180° domain walls which carry charges due to polarization discontinuity [41]. The domain configuration changes with the sweeping of the dc bias. In the vicinity of coercive voltage, the polarization is almost close to zero, which indicates a randomly oriented domains and a large domain wall density, resulting in a relatively large small signal capacitance. In the butterfly-shape hysteresis C-V curves, the two peak of capacitance correspond to two coercive voltages. Normally, the values of two coercive voltages in the C-V curve are less than that obtained from the P-V curve (shown in Fig. 3-9) perhaps because the ramping rate of dc bias voltage of C-V measurement was small than that of polarization-voltage (P-V) hysteresis measurement. Table 3-1 summarized the coercive voltage obtained from both measurements, for those capacitors annealed at various oxygen pressures. An improved symmetrically in C-V curve and a reduced coercive voltage of both curves (C-V and P-V curves) were found with decreasing oxygen pressure.

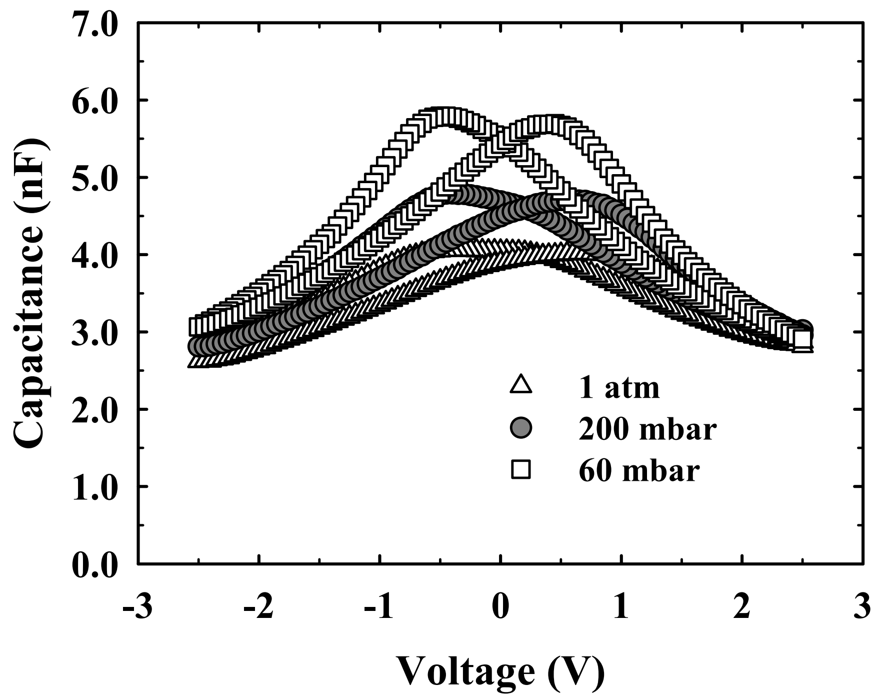

Fig. 3-8 Capacitance-voltage characteristics of the PZT thin films annealed in various oxygen pressures. The measurement frequency was kept at 100 kHz. The applied bias may be ranged from ±2.5 V and the signal level was fixed at 50 mV. All samples were annealed at 500°C for 15 min.

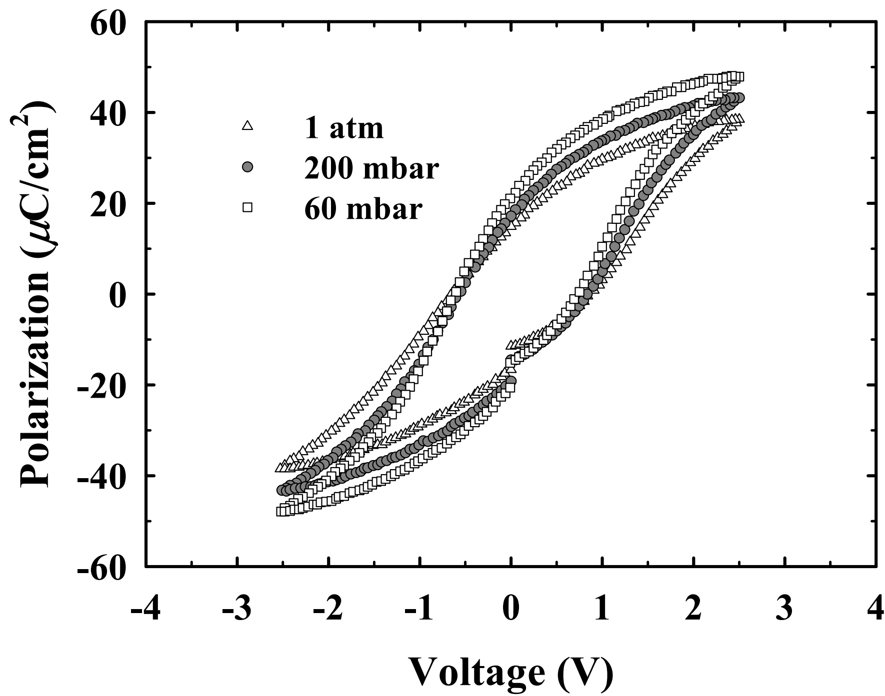

Fig. 3-9. P-V properties of the PZT thin films annealed in various oxygen pressures. The applied bias may be ranged from ±2.5 V. The frequency was around 56 Hz. All samples were annealed at 500°C for 15 min.

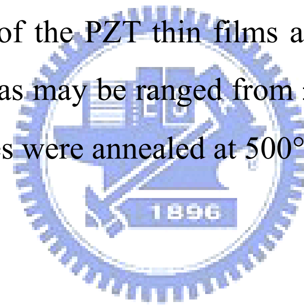

Table 3-1 The coercive voltage obtained from C-V and P-V measurements, for the Pt/$PbZr_{0.52}Ti_{0.48}O_3$/Pt capacitors annealed at various oxygen pressures.

	C-V measurement		P-V measurement	
	V_C^+ (C-V)	V_C^- (C-V)	V_C^+ (P-V)	V_C^- (P-V)
PZT thin film annealed at oxygen pressure of 1 atm	**0.65 V**	**–0.45 V**	**0.86 V**	**–0.65 V**
PZT thin film annealed at oxygen pressure of 200 mbar	**0.65 V**	**–0.40 V**	**0.83 V**	**–0.58 V**
PZT thin film annealed at oxygen pressure of 60 mbar	**0.45 V**	**–0.45 V**	**0.73 V**	**–0.62 V**

More recently, the reversible component of the polarization (P_{rev}), reported by Bolten *et al*. [06], can be expressed by the integration of C-V curve as the amplitude of the applied ac signal is sufficiently small, which does not to excite irreversible domain wall displacement.

$$P_{rev} = \frac{1}{A}\int C(V)dV, \qquad (1)$$

where A is the area of ferroelectric capacitor. Using this method, P_{rev} of those capacitors annealed at various oxygen pressures were obtained by integrating the C-V curves in Fig. 3-8, as shown in the Fig. 3-10(a). An almost straight line was found in the reversible polarizations of these films, representing to a linear dielectric constant of the ferroelectric materials. For a comparison with the reversible polarization, a large signal hysteresis loop (using RT-66A) of the capacitor annealed at oxygen pressure of around 60 mbar is shown in Fig. 3-10(b). The hysteresis loop represents the sum of reversible and irreversible polarization. In the saturation regime, the slope of P_{rev} is almost the same as that of the hysteresis loop. This is attributed to the fact that only reversible polarization occurs at this regime. The reversible polarization of the $PbZr_{0.52}Ti_{0.48}O_3$ thin films annealed at 60 mbar is around 21.33 μC/cm^2 at 2.5 V. The value is roughly half of the total polarization, giving an estimation on lattice contribution (including the electronic and ionic polarization) to the polarization [41]. Table 3-2 summarized the reversible and total polarizations obtained at 2.5 V, for those capacitors annealed at various oxygen pressures. An increase of reversible polarization was found as the oxygen pressure decreased. This trend is consistent with the results of linear dielectric constants.

Table 3-2 The reversible and total polarizations at 2.5 V, for the PZT thin films annealed at various oxygen pressures.

	Reversible Polarization (μC/cm^2)	**Total Polarization (μC/cm^2)**	**Reversible Polarization /Total Polarization**
PZT thin film annealed at oxygen pressure of 1 atm	**17.39**	**38.46**	**0.4522**
PZT thin film annealed at oxygen pressure of 200 mbar	**19.25**	**43.22**	**0.4454**
PZT thin film annealed at oxygen pressure of 60 mbar	**21.33**	**47.90**	**0.4453**

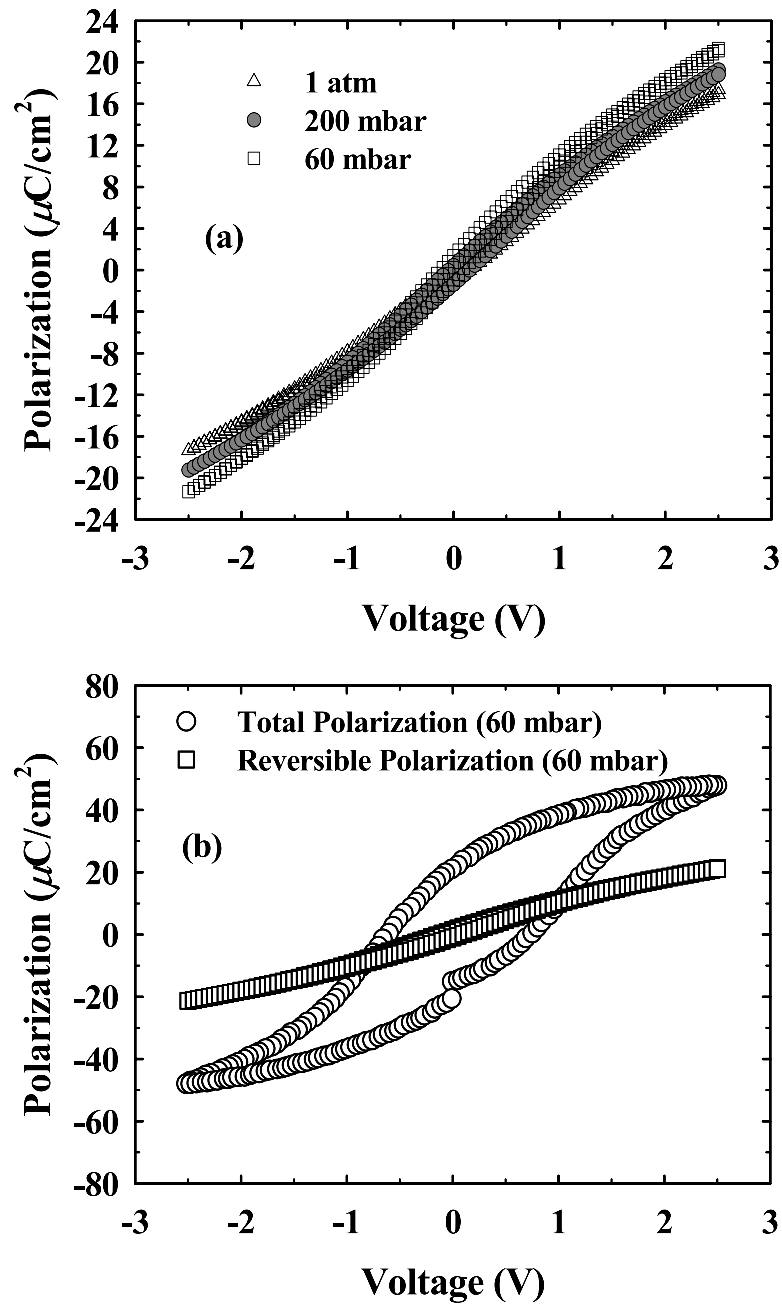

Fig. 3-10. (a) Reversible polarization of the PZT thin films annealed in various oxygen pressures. (b) Comparison of the reversible to total polarization for the sample annealed at the oxygen pressure of around 60 mbar. The reversible polarizations were obtained by integrating the C-V curves shown in Fig. 3-8.

3-3-7. Retention Property

The retention polarization of $Pt/PbZr_{0.52}Ti_{0.48}O_3/Pt$ capacitors annealed at various oxygen pressures was measured by a RT66A. The pulse widths of the write pulse and read pulse were about 2 ms and the amplitudes of both pulses were about 3.0 V. Using pulse polarization measurement, nonvolatile retention polarization can be obtained. The retention properties of those capacitors are compared and shown in Fig. 3-11. It was found that the value of retention polarization increased with decreasing the oxygen pressure. These findings indicate that low-pressure crystallization could improve the ferroelectric and dielectric properties of $Pt/PbZr_{0.52}Ti_{0.48}O_3/Pt$ capacitors at low-crystallization temperature.

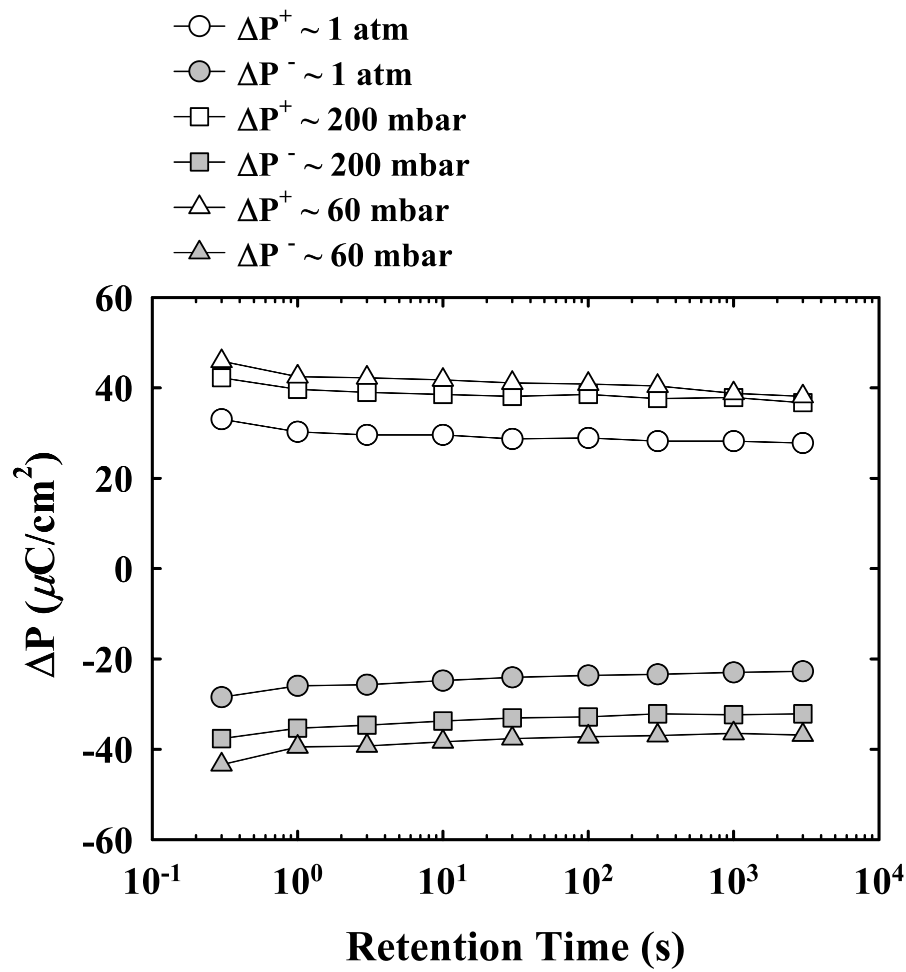

Fig. 3-11. Retention properties of the PZT thin films annealed in various oxygen pressures. The pulse width of write and read pulses were around 2 ms. The amplitudes of write and read pulses were around 3 V. All samples were annealed at 500°C for 15 min.

3-4. Summary

We have successfully demonstrated low-voltage ferroelectric characteristics suitable for embedded ferroelectric nonvolatile memory applications with the proposed one-step low-pressure oxygen annealing of $PbZr_{0.52}Ti_{0.48}O_3$ thin films. The ferroelectric properties and microstructures of $PbZr_{0.52}Ti_{0.48}O_3$ films annealed in low-pressure oxygen ambient are found to improve significantly compared with those annealed in 1 atm oxygen ambient. The improvements are ascribed to less incorporation of residues and adapted oxygen content in the resultant films, which are beneficial for complete perovskite transformation. Based on the P-E hysteresis characteristics, electrical and dielectric properties, decreasing the crystallization annealing pressure appears to be an effective method for achieving well-saturated polarization behavior at low operation voltages for $PbZr_{0.52}Ti_{0.48}O_3$ thin films.